Imaging Activation of Two Ras Isoforms Simultaneously in a Single Cell

Anna Peyker,[a] Oliver Rocks,[b] and Philippe I. H. Bastiaens*[a]

Fluorescence resonance energy transfer (FRET) microscopy approaches have been used to study protein interactions in living cells. Up to now, due to the spectral requirements for FRET detection, this has been limited to the measurement of single protein interactions. Here we present a novel time-resolved fluorescence imaging method for simultaneously monitoring the activation state of two proteins in a single cell. A Ras sensor, consisting of fluorescently labelled Ras and a fluorescently labelled Ras binding domain (RBD) of Raf, which reads out Ras activation by its interaction with RBD as a FRET signal, has been adapted for this purpose. By using yellow (YFP) and cyan (CFP) versions of the green fluorescent protein from Aquorea victoria *as donors and a tandem construct of* Heteractis crispa *Red (tHcRed) as acceptor for both donors, two independent FRET signals can be measured at the same time. Measuring the YFP and CFP donor lifetimes by fluorescence-lifetime imaging microscopy (FLIM) allows us to distinguish the two different FRET signals in a single cell. Using this approach, we show that different Ras isoforms and mutants that localize to the plasma membrane, to the Golgi or to both compartments display distinct activation profiles upon growth-factor stimulation; this indicates that there is a differential regulation in cellular compartments. The method presented here is especially useful when studying spatiotemporal aspects of protein regulation as part of larger cellular signalling networks.*

Introduction

A rapidly developing field in cell biology is that of visualizing protein interactions by using FRET microscopy. In the field of signal transduction, protein interactions are often used to monitor the activation state of signalling molecules.[1] To investigate the properties of a complex signalling network in a cell, it is crucial to be able to follow the location and timing of the activation of several protein elements of this network simultaneously as well as to correlate their activities in a cell. Small GTPases of the Ras family are key regulators in the signal-transduction networks of all eukaryotic cells. Ras family proteins work as molecular switches that cycle between an inactive GDP-bound and an active GTP-bound state in a highly regulated manner. Guanine-nucleotide exchange factors (GEFs) activate Ras proteins by exchanging GDP for GTP, whereas GTPase-activator proteins (GAPs) inactivate Ras proteins by increasing the rate of GTP hydrolysis. Each member of the Ras family has a certain subset of regulating proteins that define its activation state. In their active state, Ras proteins can bind tightly to effector molecules, which further propagate the signal. Together with the input from other signalling pathways, this regulates a variety of cellular responses, such as cell growth, survival or differentiation.

The major Ras isoforms, H-Ras, N-Ras, K-Ras4B (usually referred to as K-Ras) and the alternatively spliced K-Ras4A share a high degree of sequence homology. The sequences of the 165 N-terminal amino acids are almost identical, whereas those of the hypervariable region, consisting of the last 25 amino acids are much more dissimilar. Some regions, like the effector binding domains are 100% identical on the sequence level. H-, N- and K-Ras bind to the same set of effectors, although isoform specific preferences have been reported.[2–4] Yet, the biological output of isoform-specific signalling can be diverse. Gene knockouts of the different isoforms in mice give rise to different phenotypes.[5,6] Mutations of Ras that cause constitutive activation have been shown to be present in several cancers.[7] Analysis of human tumours has revealed a preferred occurrence of certain oncogenic Ras isoforms in certain tumour types.[8] It is still unclear how this functional specificity of Ras isoforms is achieved. Recent studies support the notion that different localization of Ras isoforms in the cell might account for their specific signalling outputs.[9] It is the very C-terminal hypervariable region of Ras that targets different Ras isoforms to different cellular locations. The only conserved motif in this region is a CAAX box (C stands for cysteine, A for an aliphatic amino acid and X for methionine or serine), a target sequence for post-translational modification. The CAAX box is recognized by a farnesyl transferase that attaches a farnesyl to the cysteine and thereby conveys an increased affinity of Ras for membranes. Subsequently the AAX residues of the CAAX motif are proteolytically removed, and the farnesylated cysteine is α-carboxymethylated by enzymes resident at the endoplasmic reticulum. An additional membrane-targeting signal then locates Ras to the plasma membrane. In the case of H- and N-Ras, this signal is palmitoylation of one or two further cysteines, respectively. K-Ras is not palmitoylated but has a polybasic domain containing multiple lysines that targets it to the plasma membrane. While K-Ras is restricted to the plasma

[a] *Mag. A. Peyker, Prof. P. I. H. Bastiaens*
European Molecular Biology Laboratory
Meyerhofstraße 1, 69117 Heidelberg (Germany)
Fax: (+49) 6221-387-242
E-mail: bastiaen@embl.de

[b] *Dipl.-Biochem. O. Rocks*
Max Planck Institute for Molecular Physiology
Otto-Hahn-Straße 11, 44227 Dortmund (Germany)

  DOI: 10.1002/cbic.200400280

membrane, N- and H-Ras also localize to the Golgi, the singly palmitoylated N-Ras to a higher content than the doubly palmitoylated H-Ras.[10]

The relevance of Ras compartmentalization has recently been addressed,[11,12] demonstrating that stimulation of a cell by epidermal growth factor (EGF) activates palmitoylated Ras isoforms not only at the plasma membrane but also at the Golgi. The activation profiles of plasma-membrane-localized Ras and of Golgi-localized Ras show different kinetics. Further studies indicate that, upon stimulation of cells, the Ras GEF Ras-GRP1 translocates to the Golgi,[13] whereas the Ras-GAP CAPRI translocates to the plasma membrane.[14] This causes a fast and transient activation of Ras at the plasma membrane and a sustained activation of Ras at the Golgi. Recently it was shown that Ras is activated at the plasma membrane, and that activation of Golgi-localized Ras occurs by net transport of Ras from the plasma membrane, independent of its activation state; this demonstrates that the activation state of Ras does not determine its subcellular localization.[10] In this work, we investigated if it is conversely the subcellular localization of Ras that causes the observed activation kinetics, by creating a signalling environment that causes transient activation at the plasma membrane but sustained activation at the Golgi. This would generate a system in which the distribution of Ras isoforms in different cellular compartments is the cause for their diverse responses.

Fluorescent biosensors for the activation of many members of the Ras family, like Rac,[15–17] Ran,[18,19] Cdc42,[20] Rap1 and Ras[21] have had a great impact on the present knowledge about their function in signal transduction. Fluorescence-based sensors for Ras activation typically contain a Ras-binding domain (RBD) of an effector protein that only interacts with the GTP-bound active form of Ras. These sensors are either used to monitor the translocation of a fluorescently labelled RBD to the sites of activated Ras or to measure FRET between a fluorescently labelled RBD and a fluorescently labelled Ras. FRET-based sensors for Ras activation can be designed as one or two polypeptides. In the first case, intramolecular binding of Ras and an RBD that are connected by a linker sequence causes a change in the FRET signal of two attached fluorophores.[21] The two-component sensor, which consists of the Ras labelled with one fluorophore and of an RBD labelled with the second fluorophore, only shows a FRET signal when Ras is activated and no signal when Ras is inactive; this gives it a very high dynamic range.[22] Studies carried out with these types of sensors have revealed important insights into real-time signalling of Ras as well as other proteins of the Ras superfamily. The major advantage of determining protein activation in single living cells as compared to large cell populations in bulk biochemical activity assays is that a level of complexity is added at the same time: the reaction of a cell towards a certain signal does not only depend on the stimulus but on the status of its internal signalling network. The fact that the status of the signalling networks in individual cells may differ makes it hard to compare the localization patterns and activation kinetics of different proteins in separate cells. To investigate the function of a Ras protein in the context of other signalling events, we developed a method that enables us to visualize the localization and activation of two proteins simultaneously in the same cell.

Results and Discussion

CFP and YFP are both FRET donors for tHcRed

FRET is a nonradiative transfer of energy from an excited donor fluorophore to an acceptor. It depends on the distance and orientation of the chromophores and on the overlap of the emission spectrum of the donor and the excitation spectrum of the acceptor.[23,24] A FRET sensor for Ras activation, which we recently developed, consists of a Ras protein fused to YFP as a donor and the Raf RBD fused to tHcRed as an acceptor.[10] In order to be able to use two sensors of this kind in a single cell, another FRET donor with a spectrum distinct from that of YFP would additionally be needed. CFP is a fluorescent protein variant with a spectrum distinct enough from YFP to separate the fluorescence signals (Figure 1). We tested whether

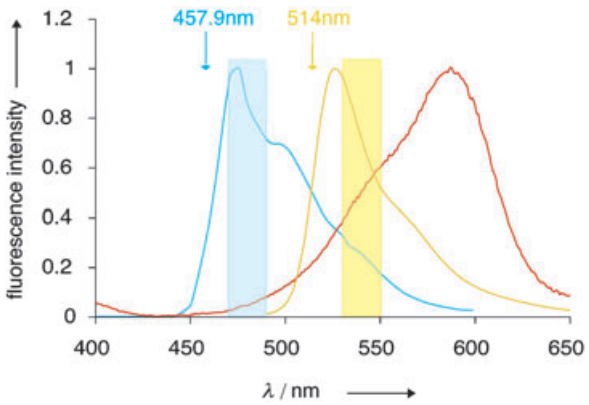

Figure 1. *Spectral overlap of CFP and YFP with tHcRed. Normalized emission spectra of CFP (cyan), YFP (Citrine, yellow) and the excitation spectrum of tHcRed (red) are shown. Arrows indicate the excitation wavelengths for CFP and YFP, the windows of fluorescence detection are shown as coloured areas. These filter settings allow separation of CFP and YFP fluorescence signals.*

the emission spectrum of CFP has a sufficient overlap with the excitation spectrum of tHcRed for efficient energy transfer (Figure 1). From the overlap of the donor emission and acceptor excitation spectra, we calculated the distance at which 50% energy transfer takes place (R_0). The R_0 of YFP and tHcRed was 6.7 nm, that of CFP and tHcRed was 4.9 nm; this clearly shows that FRET can be expected to take place not only between YFP and tHcRed but also between CFP and tHcRed and makes it possible to use these two donors simultaneously in a single cell.

We then tested if an altered version of the Ras activation sensor that uses CFP instead of YFP as a donor also gives a FRET signal in vivo. We coexpressed CFP-H-Ras and Raf-RBD-tHcRed in Maden Darby canine kidney (MDCK) cells and measured the donor lifetimes by FLIM (Figure 2). To confirm that there is energy transfer from CFP to tHcRed, we photobleach-

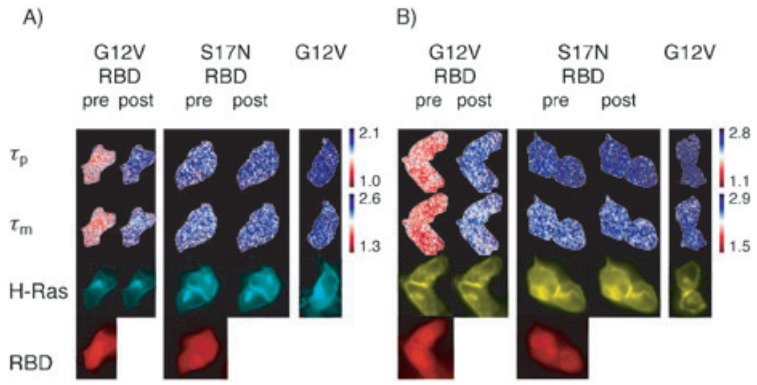

Figure 2. *CFP and YFP are FRET donors for tHcRed. The Ras activation sensor shows FRET with A) CFP- or B) YFP-Ras, indicated by an increase of donor lifetimes after acceptor photobleaching. The images show fixed cells expressing the different Ras mutants, H-Ras G12V (G12V) and H-Ras S17N (S17N) with or without the acceptor RBD-tHcRed (RBD). Fluorescence images were taken (H-Ras) and the phase (τ_p) and modulation (τ_m) lifetimes measured before (pre) and after (post) acceptor photobleaching. The lowest row shows an image of the acceptor fluorophore before photobleaching.*

ed the acceptor and compared the donor lifetimes before and after photobleaching.[25] An increase of the donor lifetime after acceptor photobleaching was observed; this demonstrates energy transfer from CFP to tHcRed (Figure 2A). To determine the maximum FRET signal that can be expected when all FRET donors are bound to an acceptor, a constitutively active mutant of H-Ras (H-Ras G12V) was used and, as a negative control, a dominant negative mutant of H-Ras (H-Ras S17N). Furthermore, the lifetime of CFP-H-Ras G12V was measured in cells expressing no acceptor. As can be seen in Figure 2, FRET only takes place in cells expressing the activated Ras mutant (G12V) and the acceptor RBD-tHcRed (RBD). No FRET occurs between the inactive mutant of Ras (S17N) and RBD-tHcRed. The lifetimes in cells that only express the donor are comparable with the lifetimes in cells expressing the dominant negative mutant or the constitutively active mutant after acceptor photobleaching. We also carried out these experiments using the same mutants of Ras, but fused to YFP, in order to compare the dynamic ranges of the FRET signals of the two sensors. Figure 2 shows a clear FRET signal with both YFP and CFP as the FRET donor. The dynamic ranges in the lifetime changes for both sensors are substantial. The average lifetime increases after acceptor photobleaching are 0.35 ns in the phase and 0.3 ns in the modulation lifetime of CFP and 0.5 ns in the phase and 0.4 ns in the modulation lifetime of YFP, in the cells expressing H-Ras G12V and RBD-tHcRed, shown in Figure 2. YFP exhibits the higher FRET efficiency in the Ras–RBD complex as expected from the R_0 values; yet these results demonstrate that both CFP and YFP can be used as FRET donors for the acceptor tHcRed.

Visualizing the activation of two different Ras proteins simultaneously

We investigated the activation profiles of plasma-membrane- versus Golgi-localized Ras using the double FRET probes in a single cell. The K-Ras isoform was used as a Ras probe that is confined to the plasma membrane, and an H-Ras mutant, H-Ras C181S, was used as a Golgi Ras probe. H-Ras C181S lacks one of its palmitoylation sites, and its steady-state distribution is therefore strongly shifted to the Golgi (Figure 3B). MDCK cells were transfected to express CFP-K-Ras, YFP-H-Ras C181S and RafRBD–tHcRed. Cells were selected that expressed all three constructs and an excess of RafRBD–tHcRed. The cells were stimulated with EGF, and the CFP and YFP lifetimes were measured over time. The average phase and modulation lifetimes

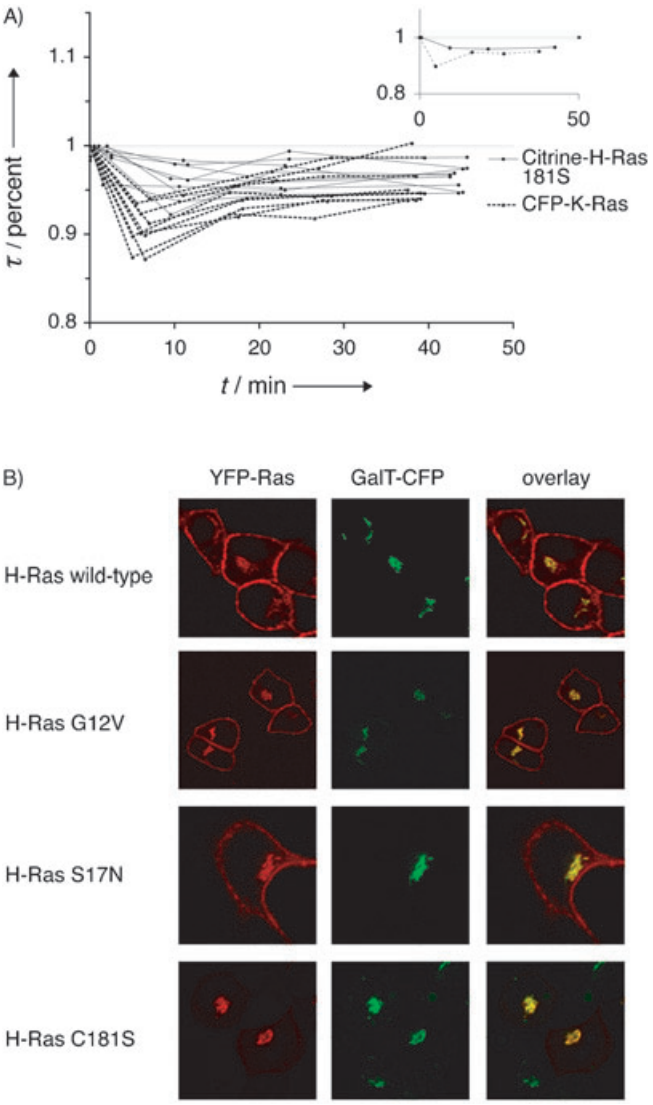

Figure 3. *Activation kinetics in single cells. A) The fluorescence lifetimes of CFP-K-Ras (broken line) and YFP-H-Ras C181S (solid line) were measured in cells expressing RBD-tHcRed. Cells were stimulated with EGF at t = 0. The normalized average of phase and modulation lifetimes (τ) obtained at each fluorescence channel was plotted against the time after EGF stimulation. In the main figure, the analysis of nine cells is displayed. The inset shows the activation profiles within a single cell at the plasma membrane and at the Golgi. B) Confocal images of cells coexpressing different H-Ras mutants labelled with YFP (YFP-Ras) in red and the Golgi marker GalT-CFP in green and an overlay image of both.*

were calculated for each fluorescence channel, and the normalized average lifetimes were displayed at each time point. Figure 3A shows the activation kinetics of nine cells, in all of which both Ras proteins responded to EGF, as judged from the decrease in fluorescence lifetime. Rapid activation of K-Ras at the plasma membrane was apparent from the drop in CFP lifetime. This activation was transient, as the lifetime increased again after reaching a minimum at 5 to 10 minutes. K-Ras displayed the same fast and transient activation profile as wild-type H-Ras at the plasma membrane, whereas H-Ras C181S displayed a sustained activation profile like wild-type H-Ras at the Golgi; this showed that the location where Ras resides in a cell does influence its activation kinetics. The drop in the YFP-H-Ras C181S lifetime after growth-factor stimulation was small; this indicates that a low amount of protein is activated. Figure 3B shows that only a very small amount of the H-Ras C181S mutant localizes to the plasma membrane as compared to wild-type H-Ras. This is in agreement with recent experiments that suggest a very short residence time of this mutant at the plasma membrane thereby decreasing the probability of its activation.[10] As seen from Figure 3A, in three out of nine cells this activation was reversible, whereas in the other six cells it stayed constant over a prolonged time. This heterogeneity in responses of individual cells, due to their individual proteomic disposition makes it difficult to compare the behaviour of different isoforms in separate cells. An illustration of the kinetics of the two Ras variants in a single cell allows a clear distinction and comparison of the two activation patterns in the same cellular conditions. The inset in Figure 3A demonstrates a delayed activation of H-Ras C181S as compared to K-Ras. This again indicates that K-Ras, due to its localization at the plasma membrane, shows the same transient activation pattern as plasma membrane localized H-Ras, whereas H-Ras C181S, due to its localization at the Golgi shows delayed and sustained activation like Golgi-localized wild-type H-Ras. The single-cell method described here thus allows us to correlate biological responses in exactly the same cellular background and makes it easier to identify cellular parameters that affect the signalling output.

Comparing multiple Ras activation kinetics within a single cell

To prove that it is the cellular location and not the isoform of Ras that determines its activation profile, the kinetics of H- and K-Ras in the plasma membrane have to be compared to the kinetics of H-Ras at the Golgi.

As the plasma membrane is a compartment where both H-Ras and K-Ras are localized, energy transfer between CFP- and YFP-labelled Ras cannot be ruled out. This could cause a problem in a case in which FRET between CFP– and YFP–Ras changes upon Ras activation. As long as such a FRET signal is constant, it would not influence lifetime changes of CFP or YFP measured upon binding of the acceptor tHcRed. To test this possibility, acceptor photobleaching experiments were performed in cells expressing different isoforms or mutants of Ras fused to CFP and YFP (Figure 4A). In all experiments, a constant increase of 0.2 ns in CFP lifetime was measured after photobleaching of the YFP. To investigate a possible effect of the isoform of Ras on the FRET signal, the photobleaching experiment was also carried out in cells expressing CFP- and YFP-labelled K-Ras (Figure 4A). The increase in CFP lifetime after photobleaching was the same as in the case of H-Ras; this excluded any influence of the isoform of Ras on the FRET signal. To rule out an influence of the activation state of Ras, photobleaching was also performed with CFP- and YFP-labelled constitutively active or dominant negative Ras (Figure 4A). Again, in both cases the lifetime increase was the same as for wild-type Ras; this showed that the FRET signal is not dependent on the activation state of Ras. To make sure that this is also the case in living cells, cells expressing CFP- and YFP-labelled H-Ras were stimulated with EGF, and the CFP lifetime was measured over time (Figure 4B). (To estimate possible effects of CFP photobleaching during the time course, four FLIM sequences were recorded before EGF addition.) The CFP lifetime did not change before or within seven minutes of EGF addition; this showed that the FRET signal stays constant when Ras gets activated in living cells. H-Ras has been reported to reside in different microdomains within the plasma membrane, depending on its activation state.[26] To test the influence of Ras membrane microlocalization on the FRET signal between two labelled Ras molecules, cells expressing CFP- and YFP-H-Ras were treated with methyl-β-cyclodextrin to disrupt plasma-membrane organization by cholesterol depletion. As shown in Figure 4B, cholesterol depletion did not influence the FRET signal between CFP- and YFP-Ras, as the CFP lifetime stayed constant over time.

tHcRed is a tandem construct of two HcRed molecules, designed to minimize dimerization of fusion proteins by forming an intramolecular dimer;[27] yet, a residual tendency of tHcRed to form oligomers cannot be excluded. Therefore crosslinking of CFP– and YFP–Ras in the plasma membrane by oligomerization of RafRBD–tHcRed was tested, as this could influence the FRET signal between CFP– and YFP–Ras. Cells expressing YFP-H-Ras, CFP-K-Ras and an excess of RafRBD–tHcRed were stimulated with EGF, and the CFP and YFP lifetimes were measured over time. To uncouple the effect of tHcRed oligomerization from its function as a FRET acceptor for CFP and YFP, tHcRed was photobleached before EGF stimulation and before each measurement of CFP or YFP lifetime. Figure 4C shows that there is no change in lifetimes of CFP or YFP and therefore no change of the constant CFP/YFP FRET signal caused by oligomerization of tHcRed. These experiments revealed a constant FRET signal between CFP- and YFP-labelled Ras proteins in the plasma membrane that is independent of activation state, isoform or membrane microlocalization of Ras and is not influenced by binding of tHcRed. This points to the presence of constitutive clusters of Ras in the plasma membrane.

In order to investigate whether the plasma membrane and the Golgi represent cellular environments that determine the activation profile of Ras isoforms, we simultaneously imaged H- and K-Ras activity in single cells to see if their activation kinetics at the plasma membrane are comparable but distinct from the activation kinetics of H-Ras on the Golgi. The known

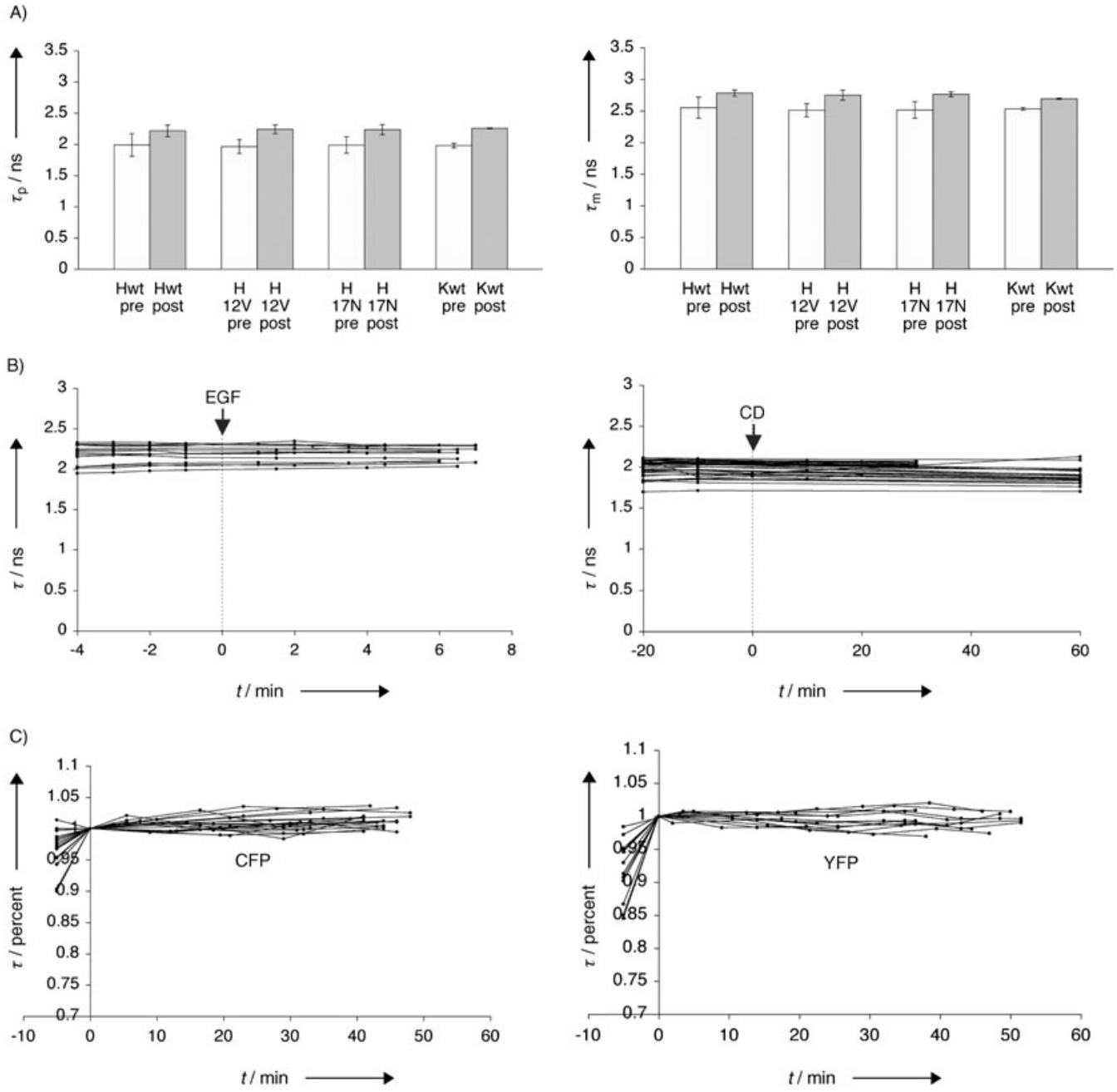

Figure 4. *FRET between CFP- and YFP-Ras in the plasma membrane. A) Cells expressing CFP- and YFP-tagged H-Ras wild-type (Hwt), H-Ras G12V (H 12V), H-Ras S17N (H 17N) or K-Ras (Kwt) were fixed, and the CFP lifetime measured before (pre) and after (post) photobleaching. A) Average phase (τ_p) and modulation (τ_m) lifetimes of at least six experiments. B) Cells expressing CFP- and YFP-H-Ras were treated with EGF or methyl-β-cyclodextrin (CD) at t = 0, and the CFP lifetimes were measured over time. The average of the phase and modulation lifetimes (τ) were plotted against the time after addition of EGF or CD. C) Cells expressing CFP-H-Ras, YFP-K-Ras and Raf-RBD-tHcRed were stimulated with EGF at t = 0. After the first lifetime measurement 5 min before addition of EGF and before each lifetime measurement, tHcRed was photobleached, and CFP and YFP lifetimes were measured over time. The averages of phase and modulation lifetimes were normalized to the lifetime value measured after photobleaching of tHcRed before addition of EGF and plotted against the time after EGF addition.*

localization of H-Ras at the plasma membrane and at the Golgi should allow discrimination of the fluorescence signals from the two locations. YFP-H-Ras wild-type, CFP-K-Ras and RafRBD–tHcRed were coexpressed in MDCK cells. After stimulation of the cells with EGF, the CFP and YFP lifetimes were measured at different time points (Figure 5). Indeed, the activation of wild-type H-Ras was much more pronounced than that of the Golgi-localized C181S mutant. Both isoforms were activated by EGF stimulation as demonstrated by a drop in lifetime, with a transient profile at the plasma membrane increasing again after a minimum at around 10 minutes (Figure 5 A). The time-dependent average lifetimes calculated for the plasma membrane and the Golgi are plotted in Figure 5 B to distinguish the activation profiles of H-Ras on the plasma membrane, H-Ras on the Golgi and K-Ras. The quantification allowed a comparison of the kinetics of H-Ras activation at the plasma mem-

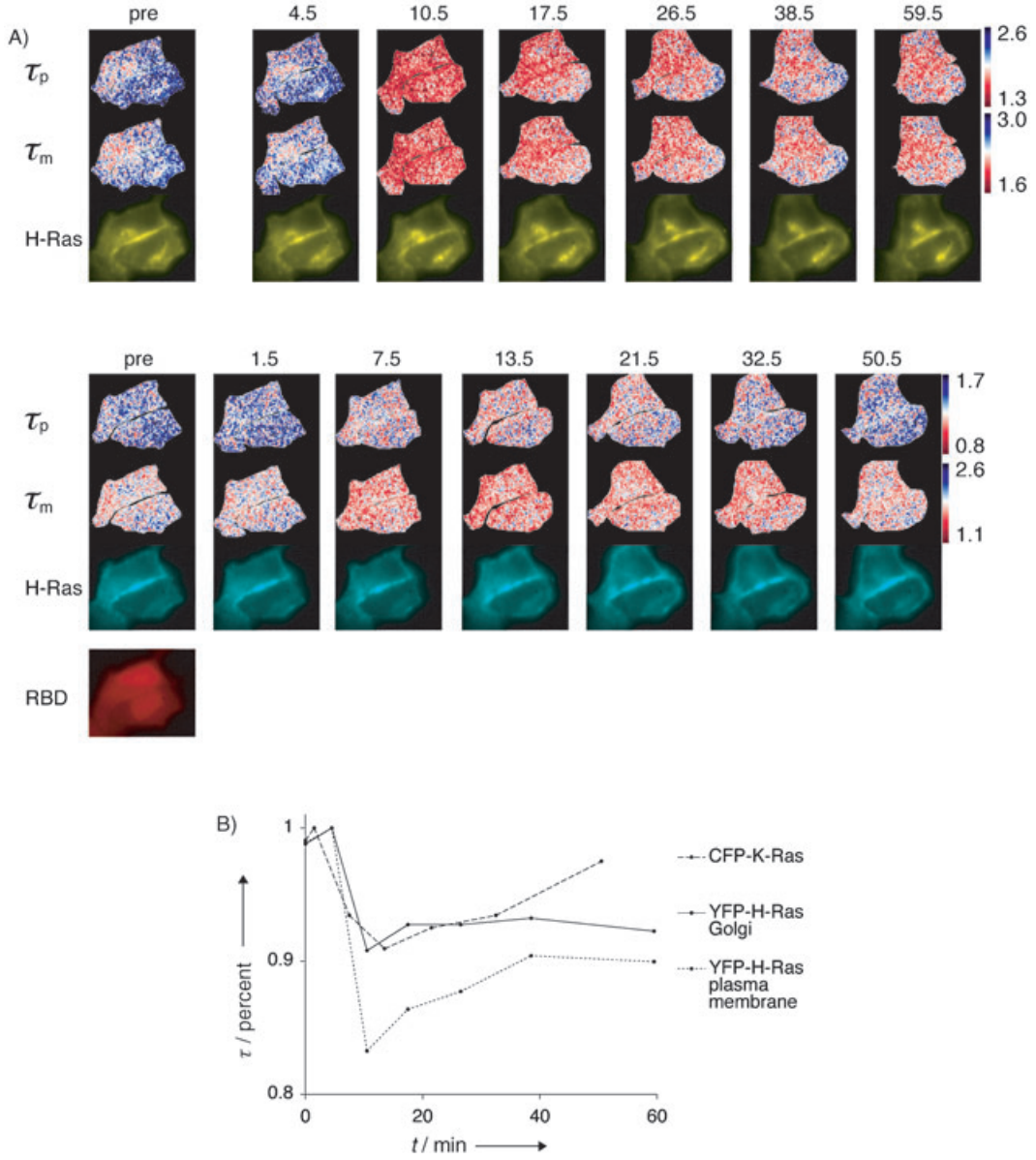

Figure 5. *Activation kinetics of H- and K-Ras. Cells expressing YFP-H-Ras, CFP-K-Ras and RBD-tHcRed were stimulated with EGF at $t=0$. Fluorescence images were taken (H-Ras, K-Ras), and the phase (τ_p) and modulation (τ_m) lifetimes were measured at the indicated time points. An image of RBD-tHcRed (RBD) was taken before EGF stimulation. B) Quantification of one of the cells shown in A. The lifetimes of Golgi-localized YFP-H-Ras (solid line), plasma membrane-localized YFP-H-Ras (dotted line) and CFP-K-Ras (broken line) were calculated, and the normalized averages of phase and modulation lifetime were plotted against the time after EGF stimulation.*

brane and at the Golgi. The onset of H-Ras activation at the Golgi was delayed compared to that at the plasma membrane. This is consistent with previous results showing that initiation of Golgi H-Ras activation occurs by net transport of active material from the plasma membrane.[10] Furthermore, H-Ras at the Golgi displayed prolonged activation in contrast to the plasma membrane, where activation was transient. This again indicates that these distinct compartments affect the activation state of Ras.

The activation kinetics of both isoforms measured in different cells exhibited similar patterns of plasma-membrane activation: fast and transient activation upon EGF stimulation. Only when the activity profiles were compared in the same cell did it become apparent that the activation of K-Ras was more reversible, whereas H-Ras exhibited a residual activity in the time window of observation. This indicates that, in addition to compartment-specific regulation of Ras isoform activity by the local composition of shared regulator molecules, the activity of Ras isoforms is subtly modulated at late time points, possibly due to sequence differences that target Ras isoforms to distinct membrane microdomains[28] that thereby influence their accessibility for regulating proteins.

Conclusion

Comparison of activation kinetics of proteins in a large number of cells bears the problem of losing information about

correlated activities due to the heterogeneity in settings of the signalling networks of cells. To circumvent this, a new FRET-based method has been used to compare multiple activation kinetics of proteins within a single cell. Two independent FRET signals were measured by FLIM, with YFP and CFP as FRET donors for the acceptor tHcRed. Using this approach, we investigated the impact that subcellular localization of different Ras isoforms has on their differential activation patterns. H-Ras, which localizes to the Golgi and to the plasma membrane, showed two different localization-dependent activation profiles upon growth-factor stimulation of the cell. Golgi-localized wild-type H-Ras displayed a similar pattern of delayed and sustained activity to a mutant that is predominantly targeted to the Golgi, whereas plasma-membrane-localized H-Ras showed the same fast and transient activity as K-Ras, an isoform that is targeted exclusively to the plasma membrane. This clearly demonstrates a dependence of the activation kinetics of Ras on its site of residence within a cell. Our results show that imaging of multiple activities in single cells can be a valuable tool to assess the spatiotemporal regulation of cellular signalling networks.

Experimental Section

Materials: Recombinant human EGF was obtained from Promega, methyl-β-cyclodextrin and reagents for cell culture were purchased from Sigma, and enzymes came from Fermentas.

Plasmids: Construction of the plasmids used in this work has been described elsewhere.[10] Citrine,[29] the YFP variant used in this work, and CFP have an additional mutation at position 206 where alanine is replaced by lysine; this is known to reduce dimerization of GFP variants.[30] GalT-CFP (Clontech) encodes a β-1,4-galactosyltransferase fused to CFP. The vectors carrying the different Ras variants originate from pEYFP and pECFP (Clontech), with the cDNA of the respective Ras version cloned into the *Xho/Bam* sites of the multiple cloning sites. The plasmid ptHcRed-C1 was a gift from J. Ellenberg. It encodes a tandem construct of two HcRed proteins, separated by the linker GAGAGAGAGAGAGPVAT. The plasmid for expression of RBD-tHcRed was constructed by cloning the DNA encoding the RBD of Raf (amino acids 52–132) into the *Xho/Bam* site of pEYFP-N1 (Clontech) and exchanging the YFP sequence for the tHcRed sequence.

Protein expression and spectroscopy: Recombinantly expressed tHcRed was obtained from Evrogen, YFP was expressed with a hexahistidine tag in *E. coli* and purified by using a Ni-NTA column (Qiagen). Spectroscopic measurements were carried out on a QuantaMaster C-61/2000SE fluorimeter (Photon Technology International). The CFP emission spectrum was obtained from fluores cence.bio-rad.com. The R_0 [nm] was calculated by using the following equation:

$$R_0 = (\kappa^2 J(\lambda) n^{-4} Q)^{1/6} \times 97$$

here κ^2 is the orientation factor, for which we assumed a value of $^2/_3$, Q is the quantum yield of the donor, which equals 0.76 for YFP (Citrine) and 0.4 for CFP (ECFP), and $J(\lambda)$ is the overlap integral of the donor emission and the acceptor excitation spectra, defined as:

$$J(\lambda) = \frac{\int F(\lambda)\varepsilon(\lambda)\lambda^4 \mathrm{d}\lambda}{\int F(\lambda)\mathrm{d}\lambda}$$

here $\varepsilon(\lambda)$ is the extinction coefficient of the acceptor, which is 160 000 $\mathrm{M^{-1}cm^{-1}}$ at 590 nm for the dimer tHcRed, and $F(\lambda)$ is the fluorescence intensity of the donor at wavelength λ. The overlap integrals were 7.745×10^{-13} $\mathrm{cm^6 mol^{-1}}$ for Citrine and tHcRed and 2.259×10^{-13} $\mathrm{cm^6 mol^{-1}}$ for ECFP and tHcRed.

Cell culture: MDCK cells were grown in Dulbecco's modified Eagle's medium (DMEM) supplemented with foetal bovine serum (10%). For live-cell microscopy, cells were grown on 35 mm glass-bottom dishes (MatTek) in low bicarbonate DMEM with HEPES (25 nM), pH 7.4 without phenol red. Cells were transfected by using the Effectene transfection kit from Qiagen. Before microscopy, cells were serum-starved for 4–8 h. To stimulate cells, EGF (100ng $\mathrm{mL^{-1}}$) was added, for cholesterol depletion, methyl-β-cyclodextrin (20 mM) was added to the imaging medium. For fixation, cells grown on cover slips were treated with paraformaldehyde (4%) at room temperature for 20 min, washed twice with PBS and twice with Tris (100 mM), NaCl (50 mM), pH 7.4, and the cover slips were mounted on glass slides in Mowiol solution (Calbiochem).

Confocal microscopy: Confocal laser scanning microscopy was performed on a Leica TCS SP2 AOBS equipped with a 63X/1.3 NA oil immersion lens and a temperature-controlled chamber. CFP and YFP were excited by using the 457.9 nm and 514 nm Ar laser, respectively.

FLIM microscopy and image processing: Experiments with fixed cells were carried out at room temperature and live-cell experiments at 37 °C. In acceptor photobleaching experiments, the acceptor was bleached to undetectable levels by prolonged irradiation (up to 4 min) with 578 nm light from a mercury lamp by using a 587/10 excitation filter. FLIM sequences were obtained at a modulation frequency of 80 MHz on an Olympus IX70 microscope by using a 100X/1.4 numerical aperture (NA) oil objective. CFP was excited with a 457.9 nm Argon laser line, and fluorescence was detected by using a dichroic beam splitter (455DCLP) and a narrow-band emission filter (HQ480/20). YFP was excited with a 514 nm Argon laser line, and fluorescence was detected with a Q530LP dichroic and a HQ538/25 emission filter. tHcRed images were recorded with a 100 W mercury arc lamp by using a 595LP dichroic filter, a 578/10 excitation filter and a D630/60 emission filter. All filters were from Chroma Technology Corp. A full description of the FLIM system and of the image processing can be found elsewhere.[31,32]

Keywords: biosensors · fluorescence · fluorescence-lifetime imaging microscopy · FRET · Ras

[1] F. S. Wouters, P. J. Verveer, P. I. Bastiaens, *Trends Cell. Biol.* **2001**, *11*, 203.
[2] A. B. Walsh, D. Bar-Sagi, *J. Biol. Chem.* **2001**, *276*, 15 609.
[3] J. Yan, S. Roy, A. Apolloni, A. Lane, J. F. Hancock, *J. Biol. Chem.* **1998**, *273*, 24 052.
[4] P. Rodriguez-Viciana, C. Sabatier, F. McCormick, *Mol. Cell. Biol.* **2004**, *24*, 4943.
[5] L. M. Esteban, C. Vicario-Abejón, P. Fernández-Salguero, A. Fernández-Medarde, N. Swaminathan, K. Yienger, E. Lopez, M. Malumbres, R. McKay, J. M. Ward, A. Pellicer, E. Santos, *Mol. Cell. Biol.* **2001**, *21*, 1444.
[6] L. Johnson, D. Greenbaum, K. Cichowski, K. Mercer, E. Murphy, E. Schmitt, R. T. Bronson, H. Umanoff, W. Edelmann, R. Kucherlapati, T. Jacks, *Genes Dev.* **1997**, *11*, 2468.
[7] M. Barbacid, *Annu. Rev. Biochem.* **1987**, *56*, 779.
[8] J. L. Bos, *Cancer Res.* **1989**, *49*, 4682.
[9] J. F. Hancock, *Nat. Rev. Mol. Cell Biol.* **2003**, *4*, 373.

[10] O. Rocks, A. Peyker, M. Kahms, P. J. Verveer, C. Koerner, M. Lumbierres, J. Kuhlmann, H. Waldmann, A. Wittinghofer, P. H. Bastiaens, *Science*, in press.
[11] V. K. Chiu, T. Bivona, A. Hach, J. B. Sajous, J. Silletti, H. Wiener, R. L. Johnson II, A. D. Cox, M. R. Philips, *Nat. Cell Biol.* **2002**, *4*, 343.
[12] I. Perez de Castro, T. G. Bivona, M. R. Philips, A. Pellicer, *Mol. Cell. Biol.* **2004**, *24*, 3485.
[13] T. G. Bivona, I. Perez de Castro, I. M. Ahearn, T. M. Grana, V. K. Chiu, P. J. Lockyer, P. J. Cullen, A. Pellicer, A. D. Cox, M. R. Philips, *Nature* **2003**, *424*, 694.
[14] P. J. Lockyer, S. Kupzig, P. J. Cullen, *Curr. Biol.* **2001**, *11*, 981.
[15] M. A. Del Pozo, W. B. Kiosses, N. B. Alderson, N. Meller, K. M. Hahn, M. A. Schwartz, *Nat. Cell Biol.* **2002**, *4*, 232.
[16] V. S. Kraynov, C. Chamberlain, G. M. Bokoch, M. A. Schwartz, S. Slabaugh, K. M. Hahn, *Science* **2000**, *290*, 333.
[17] E. Tzima, M. A. Del Pozo, W. B. Kiosses, S. A. Mohamed, S. Li, S. Chien, M. A. Schwartz, *EMBO J.* **2002**, *21*, 6791.
[18] K. Plafker, I. G. Macara, *J. Biol. Chem.* **2002**, *277*, 30121.
[19] P. Kalab, K. Weis, R. Heald, *Science* **2002**, *295*, 2452.
[20] R. E. Itoh, K. Kurokawa, Y. Ohba, H. Yoshizaki, N. Mochizuki, M. Matsuda, *Mol. Cell. Biol.* **2002**, *22*, 6582.
[21] N. Mochizuki, S. Yamashita, K. Kurokawa, Y. Ohba, T. Nagai, A. Miyawaki, M. Matsuda, *Nature* **2001**, *411*, 1065.
[22] A. R. Reynolds, C. Tischer, P. J. Verveer, O. Rocks, P. I. Bastiaens, *Nat. Cell Biol.* **2003**, *5*, 447.
[23] T. Förster, *Ann. Phys.* **1948**, *2*, 57.
[24] R. M. Clegg, *Fluorescence Resonance Energy Transfer*, Wiley, New York, **1996**.
[25] P. I. Bastiaens, I. V. Majoul, P. J. Verveer, H. D. Soling, T. M. Jovin, *EMBO J.* **1996**, *15*, 4246.
[26] I. A. Prior, A. Harding, J. Yan, J. Sluimer, R. G. Parton, J. F. Hancock, *Nat. Cell Biol.* **2001**, *3*, 368.
[27] D. Gerlich, J. Beaudouin, B. Kalbfuss, N. Daigle, R. Eils, J. Ellenberg, *Cell* **2003**, *112*, 751.
[28] I. A. Prior, J. F. Hancock, *J. Cell Sci.* **2001**, *114*, 1630.
[29] O. Griesbeck, G. S. Baird, R. E. Campbell, D. A. Zacharias, R. Y. Tsien, *J. Biol. Chem.* **2001**, *276*, 29188.
[30] D. A. Zacharias, J. D. Violin, A. C. Newton, R. Y. Tsien, *Science* **2002**, *296*, 913.
[31] A. Squire, P. I. Bastiaens, *J. Microsc.* **1999**, *193*(1), 36.
[32] A. Squire, P. J. Verveer, P. I. Bastiaens, *J. Microsc.* **2000**, *197*(2), 136.

Received: August 4, 2004

